roductory Remarks

the most rudimentary aspects of the electronic theory and interactions of molecular oxygen and the interpretation of reactivities of singlet and triplet oxygen by the organic chemist.

We hope that this gap will be overcome in part by this volume and that a further enhancement of the mechanistic understanding of the interaction of oxygen with other molecules will ensue.

#### MICHAEL KASHA

#### REFERENCES

Ihde, Aaron J. (1961). "The Development of Modern Chemistry," pp. 40-54. Harper, New York.

Schaap, A. Paul (1976). "Singlet Molecular Oxygen." Dowden, Hutchinson, and Ross, Inc., Stroudsburg, Pennsylvania. 1

# Singlet Oxygen Electronic Structure and Photosensitization

# MICHAEL KASHA and DALE E. BRABHAM

T	Introduction		1
TT	Primitive Representations of Oxygen Molecule States		2
***	A. Lewis Structures for O <sub>2</sub>		2
	B. Primitive Molecular Orbital Representations of O <sub>2</sub> States		3
ш	Real and Complex Orbitals for O <sub>2</sub>		4
	A. The Real $\pi$ Orbitals for the Oxygen Molecule		5
	B. The Complex $\pi$ Orbitals for the Oxygen Molecule		8
IV.	The Molecular State Functions for O <sub>2</sub>		12
:	A. The Molecular Orbital Configuration for Molecular Oxygen		12
	B. Spin and Orbital Angular Momenta for π Orbital Assignment	ts .	14
	C. Construction of Determinantal Wave Functions for $\pi$ Electro	n	
	States of O <sub>2</sub>		16
	D. Electron Repulsion in the $\pi$ Electron States of $O_2$		18
	E. Degeneracies in the $\pi$ Electron States of $O_2$		20
	F. The Real $\pi$ Electron State Functions for $O_2$		22
	G. The Literature on Molecular Oxygen Structure		2
v	Sensitization Mechanisms for Singlet Oxygen		2
	. Summary		3
* 1	References		3:

#### I. INTRODUCTION

This chapter presents a discussion of the structure of molecular oxygen in its various lowest electronic states, and relates these structures to spectra, chemical reactivity, and sensitization mechanisms. The presentation is intended to serve as a bridge between the most primitive representations and the simplest adequately sophisticated ones.



Fig. 1. Potential energy curves for molecular oxygen (after Herzberg, 1950).

Molecular oxygen, considered as a normal or ground state chemical species has been the subject of research for two centuries. As a physical species, research has centered on spectroscopic observations especially in reference to excited states which affect optical transmission of the earth's atmosphere. The last decade and a half has brought a new vigorous phase to oxygen research: the chemical reactivities of excited states of molecular oxygen, a phase of research promoted by the strong interaction of spectroscopic and chemical researches.

The potential energy diagram for the lowest electronic states of molecular oxygen is depicted in Fig. 1 (after Herzberg, 1950). The strongly allowed absorption  ${}^3\Sigma_u - \leftarrow {}^3\Sigma_g - is$  known to spectroscopists as the Schumann-Runge band system with an origin at  $\sim 2026 \, \text{Å}^-$  (49363 cm<sup>-1</sup>), thereby giving the UV limit to atmospheric transmission. A forbidden transition  ${}^3\Sigma_u + \leftarrow {}^3\Sigma_g - i$  (not shown in Fig. 1) is known as the Herzberg band system, and has an origin at  $\sim 2800 \, \text{Å}$  (35713 cm<sup>-1</sup>).

# II. PRIMITIVE REPRESENTATIONS OF OXYGEN MOLECULE STATES

## A. Lewis Structures for O2

It is the low-lying singlet excited states of oxygen on which most of the new interest is focused (cf. Fig. 1). The first qualitative discussion of oxygen electronic structure was given by G. N. Lewis (1916) in his paper, "The Atom and the Molecule," in which electron-paired and diradical "structures" of oxygen and ethylene were discussed: "These two forms of oxygen (which, of course, may merge into one another by continuous gradations) can be represented by

and the two forms of ethylene as

It is still generally assumed today that these Lewis structures correspond to "singlet" and "triplet" electron configurations. Lewis (1924a,b) later added further commentary to indicate localization of the "odd" electrons in the diradical form in which "one of the bonds is broken in such a way as to be equally divided between the two atoms, so that each atom possesses an odd electron," which recently was appraised as "a suggestion that in qualitative terms still adequately describes the ground state of molecular oxygen." In this chapter it will be shown that this is not an acceptable appraisal. Lewis (1924a,b) in this later paper modified his earlier concept of gradual tautomerization: "The enormous difference in magnetic properties between the oxygen molecule and other molecules to which we attribute double bonds seems to support the idea that the change from a nonmagnetic to a magnetic molecule is not a gradual process, but that the molecule must possess at least one unit of magnetic moment or no magnetic moment at all."

We have quoted extensively from Lewis' writings on molecular oxygen not to criticize their conceptual character for their time, but to point up their inadequacy for mechanistic deductions today. Yet in spite of a far deeper understanding of the rudiments of electronic structure of molecular oxygen now available, researchers in the forefront of triplet and singlet molecular oxygen reactions still rely on utterly inappropriate primitive representations for the problem. On the other hand, chemical physicists have not made it easy for the experimentalist to refine his models, so the need for a simple and fresh new exposé of the details of molecular electronic structures of various molecular oxygen states is quite pressing. We are devoting the first half of this chapter to this problem.

# B. Primitive Molecular Orbital Representations of O2 States

Primitive representations of the three lowest electronic states of molecular oxygen are reproduced in Fig. 2. The first column indicates the diatomic molecule state designations familiar now at least as labels to most researchers

STATE	ORBITAL ASSIGNMENT	LEWIS STRUCTURE	WAVE FUNCTION
$^{t}\Sigma_{g}^{+}$	$\bigcirc_{\pi_{x}}\bigcirc_{\pi_{y}}$	:Ö: Ö:	$\pi_{x}(1) \alpha(1) \pi_{y}(2) \beta(2)$
¹∆g	$\bigcirc_{\pi_{\mathbf{x}}}\bigcirc_{\pi_{\mathbf{y}}}$	:Ö: Ö:	$\pi_{\rm g}$ (1) Q(1) $\pi_{\rm g}$ (2) $\beta$ (2)
$^3\Sigma_g^-$	$\bigcirc_{\pi_{x}}\bigcirc_{\pi_{y}}$	:Ö : Ö:	$\pi_{x}(1) \alpha(1) \pi_{y}(2) \alpha(2)$

Fig. 2. Primitive representations of molecular oxygen lowest singlet and triplet states.

dealing with molecular oxygen. We shall return to the significance of these state symbols later. Column 2 of Fig. 2 depicts what many chemists use and believe to represent the orbital assignment of electrons for the three lowest electronic states of molecular oxygen. The two circles represent "cells" of electron orbital occupancy, the orbital designations corresponding to the real molecular antibonding, degenerate (i.e., equal energy)  $\pi$  orbitals  $(2p_x\pi_g$  and  $2p_y\pi_g$ , or serially,  $1\pi_g^x$  and  $1\pi_g^y$ ; or  $\pi_x$ ,  $\pi_y$ ) for diatomic molecules familiar to most chemists today (cf. Fig. 5, top line). These simple diagrammatic resolutions of Fig. 2, which seem so clearly to delineate pronounced differences in electronic orbital assignments for the three states of O2, lend a false sense of security in that they simply do not correspond to the oxygen molecule states, even though they appear to do so with transparent clarity. Why are these simple pictures so inadequate? From one point of view, the diagrams seem to suggest three state configurations, one  ${}^{1}\Sigma_{g}^{}^{}^{}$ , one  ${}^{1}\Delta_{g}^{}$ , and one  ${}^{3}\Sigma_{g}^{-}$  when the actual numbers are one, two, and three, respectively; we must, therefore, have a proper representation for these states and their correct number.

From another point of view, the wave functions (last column of Fig. 2) which describe these configurations are seen to be incorrect for the description of electron distribution functions. {In these wave functions,  $\pi_x$  and  $\pi_y$  represent the real degenerate pair for the configuration shown in Fig. 5 [top line: ...  $(1\pi_g)^2$ ], (1) and (2) represent electron labeling, and  $\alpha$  and  $\beta$  represent spin-up, spin-down spin functions with spin angular momentum eigenvalues  $+(1/2)(h/2\pi)$  and  $-(1/2)(h/2\pi)$ }. These wave functions are inadequate because they fail to take into account electron indistinguishability (interchanges of indices 1 and 2) and also because the functions are symmetric under electron interchange, whereas proper electron wave functions are antisymmetric under electron interchange (the two-electron wave functions should change sign when 1 and 2 are interchanged). So these overall

electron wave functions are incorrect, and cannot correspond to the apparent distinctions suggested by the cell diagrams of column 2, Fig. 2.

The (spin-designated) Lewis structures (column 3, Fig. 2) corresponding to the cell diagrams of column 2 can be criticized on even further grounds:

(a) The Lewis structures designate electron localization on each atom, whereas the cell diagrams at least indicate occupancy of molecular orbitals delocalized with respect to the two oxygen atoms of the molecule. (b) The Lewis structures also incorporate the inadequacies of the cell diagrams, enumerated above. (c) The Lewis structures seem to impart a "nonbonding" electron role to four pairs of valency electrons; these assigned roles contrast to the bonding and antibonding roles of all the valency electrons designated by even the simplest molecular orbital picture (described later).

# III. REAL AND COMPLEX ORBITALS FOR O2

# A. The Real $\pi$ Orbitals for the Oxygen Molecule

In this section we shall discuss the form of the real and complex orbitals (Fig. 3) involved in building up the configuration of molecular oxygen. The diagrams of Fig. 3 represent schematic boundary surfaces for 90% of the electron probability, the contour lines merely indicating the three-dimensional shape of the boundary surface. As the well-known simple molecular orbital configuration of molecular oxygen indicates (top line of Fig. 5), all of the orbitals are fully occupied except the last pair,  $1\pi_g$ , each of which is half filled. This  $1\pi_g$  orbital exists in two equal energy (or degenerate) forms, and only two electrons are available for populating the  $1\pi_g$  pair.

The real molecular orbitals are shown on the left side of Fig. 3 and are universally known as the  $\pi$ -bonding molecular orbital  $(2p_x\pi_u)$  and the  $\pi$ -antibonding molecular orbital  $(2p_x\pi_g)$ , totally familiar from examples in C=C bonds. These orbitals are expressible as first approximations by linear combinations of atomic orbitals for the component atoms.

$$(2p_x\pi_u) \equiv (1\pi_u^x) = \frac{1}{\sqrt{2}}(\phi_{2p_x} + \phi_{2p_x})$$

$$(2p_x\pi_g) \equiv (1\pi_g^x) = \frac{1}{\sqrt{2}}(\phi_{2p_x}, -\phi_{2p_x})$$

It is clear that the signs of the linear combinations indicate constructive interference (+ combination) of the two atomic wave functions and thus bonding for the  $1\pi_u^x$  orbital, and destructive interference (- combination)

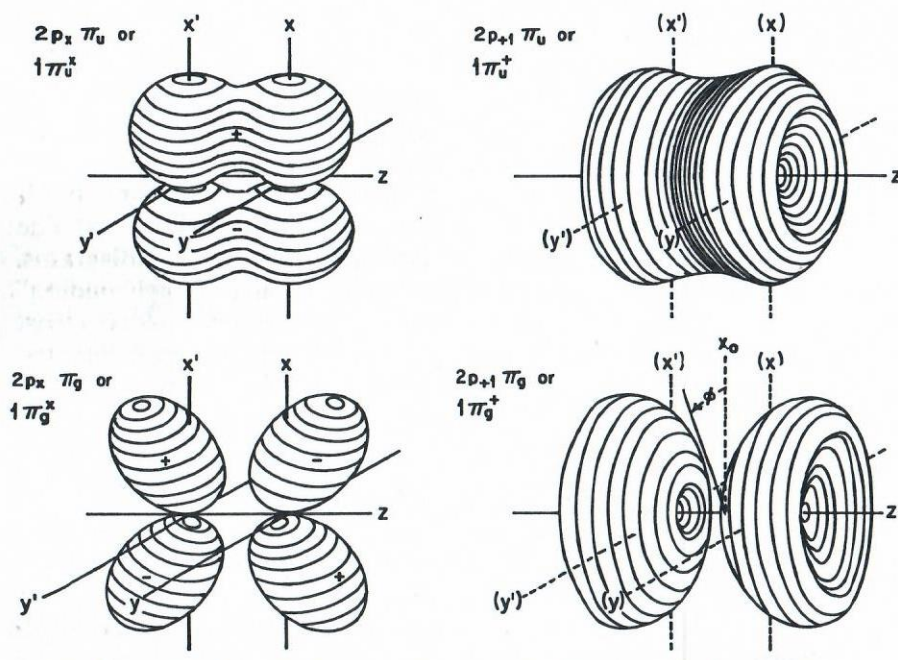


Fig. 3. Real and complex bonding and antibonding diatomic molecule  $\pi$  orbitals, showing boundary contour surface.

of the two atomic wave functions and thus antibonding between the two atoms (for the  $1\pi_{\sigma}^{x}$  orbital).

There is another set of y axis oriented  $\pi$  orbitals which may be expressed analogously.

$$(2p_y\pi_u) \equiv (1\pi_u^y) = \frac{1}{\sqrt{2}}(\phi_{2p_y}, + \phi_{2p_y})$$

$$(2p_y\pi_g) \equiv (1\pi_g^y) = \frac{1}{\sqrt{2}}(\phi_{2p_y} - \phi_{2p_y})$$

Three simple observations can be made concerning the orbitals just described:

- (a) The  $1\pi_u^x$  and  $1\pi_u^y$  orbitals and the  $1\pi_g^x$  and  $1\pi_g^y$  orbitals form exactly equivalent pairs (equal energy, degenerate). Thus, they each require double-electron occupancy, or a total of four electrons for closed-shell configurations.
- (b) Each electron in a  $\pi_u$  or  $\pi_g$  orbital is fully delocalized with respect to the atomic centers, e.g., the Fig. 3 patterns are one-electron wave functions,

or (mathematical, nonobservable) electron distribution functions; the square of these wave functions gives the point probability density for finding an electron (which is, in principle, a physical or observable quantity).

(c) The inversion operation î applied to the  $\pi_u$  function (point by point) clearly converts it into  $-(\pi_u)$  (therefore it is designated u for *ungerade*, or odd, under inversion) whereas  $\pi_g$  under operator î goes to  $+(\pi_g)$  (thus g

for gerade, or even, under inversion).

There is another observation which now must be made concerning the real form of the orbitals. The chemist feels naturally at home in real Cartesian space, but does the oxygen molecule? The answer is a qualified no. In the free molecule there is certainly a physical operational significance to the interatomic axis (the z axis in Fig. 3), but in the free molecule there is no operational significance to the x or y axes, i.e., the xz and yz planes are not operationally defined. Therefore, it may be mathematically convenient for some purposes to use Cartesian coordinate orbital resolution, but we must remember that the  $\pi^x$  and  $\pi^y$  orbitals act as pairs and not as separate orbitals. This is clearly indicated by the symmetry operators. It was shown that inversion, î, transforms each  $\pi$ -type into itself or its negative, but this is not true of other symmetry operators. For example, the reflection operator in a plane containing the z axis  $(\hat{\sigma_v})$  would at first sight send  $(1\pi_v^x)$ into  $-(1\pi_u^x)$  and  $(1\pi_g^x)$  into  $-(1\pi_g^x)$  (the common concept of " $\pi$ -antisymmetry"). But this application of  $\hat{\sigma}_{v}$ , while perfectly applicable to ethylene  $\pi$ -bonds with a defined yz plane for the molecular skeleton, does not apply to a diatomic molecule. In a diatomic molecule the reflection plane  $\hat{\sigma_v}$  may have any arbitrary orientation in space as long as it contains z (thus, the  $D_{mh}$  point group table indicates  $\infty \sigma_{v}$ ; if  $\hat{\sigma_{v}}$  is chosen to bisect the xz and yz planes, and is applied to  $\pi_u^x$ , a combination of  $\pi_u^x$  and  $\pi_u^y$  results. This intertransforming characteristic is another manifestation of  $\pi_u^x$  and  $\pi_u^y$ orbital degeneracy. A similar result obtains even more irretrievably with the operator  $\hat{C}_{\phi}$ , rotation by an (arbitrary) angle about the z axis. If the orbital  $\pi_u^x$  is rotated by any one of the infinite number  $(\infty C_\phi)$  of arbitrarily chosen angles  $\phi$ ,  $\pi_u^x$  always goes into some combination of  $\pi_u^x$  and  $\pi_u^y$ ; only if  $\phi$  is chosen to be 180° does  $(1\pi_u^x)$  go into  $-(1\pi_u^x)$ ; that exclusive choice, however, is not permitted for the cylindrically symmetrical  $(D_{coh})$ molecule.

Similar deductions concerning the interdependence of the pair of real orbitals  $\pi_x$  and  $\pi_y$  are obtained if we consider angular momentum operators for the  $O_2$  molecule. The net conclusion is that the real orbital resolution has only a mathematical and not an operational significance for the free molecule.

There is, however, a circumstance in which the real orbitals gain an operational significance and that is when the  $O_2$  molecule is approached

9

by an interacting or reacting molecule. Then the Cartesian axes and corresponding perpendicular planes gain physical meaning. Griffith (1964a,b) has utilized this resolution in predicting hydration effects in the  $\rm O_2$  molecule, and Kearns (1969) and others have used this resolution in discussion of reaction mechanisms, e.g., oxygen-ethylene correlation diagrams. So one could say that resolution of molecular oxygen orbitals into real Cartesian components "prepares" the molecule for perturbation effects in a Cartesian (cubic or octahedral) field.

## B. The Complex $\pi$ Orbitals for the Oxygen Molecule

The complex  $\pi$  orbitals (Fig. 3) are less familiar to the chemist, yet they are just as simply described as the real orbitals and have direct operational significance for the free molecule (uniaxial field defined by its own interatomic coordinate, the z axis). Actually the complex functions in atoms (full rotation group, with spherical polar coordinates r,  $\theta$ ,  $\phi$ ) and in homonuclear diatomic molecules ( $D_{\infty h}$  infinite point group, cylindrical coordinates, r, z,  $\phi$ ) are derived naturally (in principle) from the wave mechanical solution, and then transformed into real Cartesian functions secondarily. The reason for the latter step in atoms is the same as that just described above; it is not that, e.g.,  $p_x$ ,  $p_y$ , and  $p_z$  are operationally defined in a free atom, it is that we prepare the atom in a triaxial Cartesian field for interactions with other atoms for molecule formation; it is the approaching perturbing atoms which may give  $p_x$ ,  $p_y$ , and  $p_z$  operational significance.

Hence, since we have discussed the familiar real  $\pi$  orbitals first, we shall now reverse the normal process and essentially convert the real molecular wave functions back into the complex functions. The transformation is simple, and is mathematically identical to the resolution of circularly polarized light into plane (perpendicularly) polarized components  $P_x$  and  $P_y$ , or resolution of a plane polarized component, say  $P_x$ , into  $P_+$  and  $P_-$  right and left circularly polarized components. The transformation equation is one of the Euler relations

$$e^{+i\phi} = \cos \phi + i \sin \phi$$
  
 $e^{-i\phi} = \cos \phi - i \sin \phi$ 

We shall compare the transformation of real and complex orbitals for atoms with the transformation for diatomic molecules. The element in common for these is that for spherical polar coordinates in atoms the polar angle  $\phi$ , for the  $2\pi$  rotation about a z axis chosen as reference, is analogous to the axial  $2\pi$  rotation angle  $\phi$  about the z axis chosen as reference for diatomic molecules.

# 1. Transformation of the Real 2p Orbitals to Complex 2p Orbitals for Atoms

The real 2p atomic orbitals may be written

$$2p_{x} = xR(r) = r \sin \theta \cos \phi R(r)$$

$$2p_{y} = yR(r) = r \sin \theta \sin \phi R(r)$$

$$2p_{z} = zR(r) = r \cos \theta \cdot 1 \cdot R(r)$$

where the real  $\Phi(\phi)$  functions are italicized for emphasis. If we consider an atom in a uniaxial field, such as a magnetic field, chosen to coincide with the z axis, we could apply the angular momentum operator

$$\hat{p_{\phi}} = \frac{h}{2\pi i} \frac{\partial}{\partial \phi}$$

to obtain the units of angular momentum (orbital angular momentum eigenvalue) corresponding to each 2p orbital. Taking the simple partial derivative with respect to  $\phi$ 

$$\frac{h}{2\pi i} \frac{\partial}{\partial \phi} (xR) = -\frac{h}{2\pi i} (r \sin \theta \sin \phi) R = (+i) \frac{h}{2\pi} (yR)$$

$$\frac{h}{2\pi i} \frac{\partial}{\partial \phi} (yR) = \frac{h}{2\pi i} (r \sin \theta \cos \phi) R = (-i) \frac{h}{2\pi} (xR)$$

$$\frac{h}{2\pi i} \frac{\partial}{\partial \phi} (zR) = \frac{h}{2\pi i} (r \cos \theta \cdot 0) R = (0) \frac{h}{2\pi} (zR)$$

we do not get eigenvalue equations, but find that the real x and y functions transform into each other instead of into themselves.

However, if we use the linear combinations\* (the real functions being normalized)

$$p_{+} = \frac{1}{\sqrt{2}}(p_{x} + ip_{y})$$
$$p_{-} = \frac{1}{\sqrt{2}}(p_{x} - ip_{y})$$

and then apply the Euler relations, we obtain complex atomic orbitals

<sup>\*</sup> This particular linear combination  $(1p_x + ip_y)$  is chosen to permit the application of the Euler relation instead of, e.g.,  $1p_x + 1p_y$ .

which are eigenfunctions of  $p_{\phi}$ ,

$$p_{+1} = r \sin \theta e^{+i\phi} R(r)$$
$$p_{-1} = r \sin \theta e^{-i\phi} R(r)$$

$$p_0 = r \cos \theta \, e^{0\phi} \, R(r)$$

with eigenvalues +1, -1, and 0  $(h/2\pi)$ , respectively.

#### 2. Transformation of Real $\pi$ Orbitals to Complex $\pi$ Orbitals for Diatomic Molecules

Now we are in a position to compare the analogous result for diatomic molecular orbitals. As indicated earlier, the diatomic orbitals may in first approximation be written as linear combinations of atomic orbitals

$$\pi_{g}^{x} = \frac{1}{\sqrt{2}} (2p_{x'} - 2p_{x})$$

$$\pi_{g}^{y} = \frac{1}{\sqrt{2}} (2p_{y'} - 2p_{y})$$

The  $\Phi(\phi)$  functions for diatomic molecular orbitals and for orbitals for the free atoms are identical,  $\Phi(\phi) = (1/\sqrt{\pi})e^{im_1\phi}$ .

Now the presence of a uniaxial field (z axis) is imposed by the molecular structure and does not depend on the imposition of an external field. Consequently, the  $\pi$  orbitals for the molecule should be eigenfunctions of the  $p_{\phi}$  operator. However, as in the case of atoms, the real orbital components of the molecular orbitals will transform  $x \to y$  and  $y \to x$ , so the real  $\pi$  orbitals separately do not behave properly as eigenfunctions.

Taking linear combinations of the real  $\pi$  orbitals, we construct the complex  $\pi$  orbitals as follows

$$\pi_{\rm g}^{+1} = \frac{1}{\sqrt{2}} (\pi_{\rm g}^{\ x} + i\pi_{\rm g}^{\ y})$$

$$\pi_{\rm g}^{-1} = \frac{1}{\sqrt{2}} (\pi_{\rm g}^{\ x} - i\pi_{\rm g}^{\ y})$$

These orbitals may then be written, by the Euler relation, as

$$\pi_{\rm g}^{+1} = Z_{-}(z) R(r) e^{+i\phi}$$

$$\pi_{\rm g}^{-1} = Z_{-}(z) R(r) e^{-i\phi}$$

The 2p<sub>z</sub> and 2p<sub>z</sub> orbitals, which we have not mentioned, were used to form

the  $2p_z\sigma_g$  and  $2p_z\sigma_u$  sigma bonding and antibonding orbitals (labeled serially  $3\sigma_g$  in Fig. 5, first line). It is now simply demonstrable that

$$\hat{p_{\phi}}(\pi_{g}^{+1}) = (+1)\frac{h}{2\pi}(\pi_{g}^{+1})$$

$$\hat{p_{\phi}}(\pi_{g}^{-1}) = (-1)\frac{h}{2\pi}(\pi_{g}^{-1})$$

so that the complex  $\pi$  orbital functions are indeed eigenfunctions of the appropriate angular momentum operator. We may attribute the +1 and  $-1(h/2\pi)$  units of angular momenta to clockwise and counterclockwise electron currents about the z axis (analogous to the concept of circular polarization of light).

#### 3. Symmetry Properties of the Complex $\pi$ Orbitals

Structure and Sensitization

Now a question of interest is, how can we picture these complex orbitals. We may use the modulus of a complex function

$$|\Phi_{+1}^*\Phi_{+1}| = |e^{-i\phi}e^{i\phi}| = 1$$

which indicates that the function in real space has a constant numerical value as a function of  $\phi$ , i.e., a unit circle gives the real spatial  $\phi$  dependence of the orbitals  $\pi_g^{+1}$ ,  $\pi_g^{-1}$ ,  $\pi_u^{+1}$ , and  $\pi_u^{-1}$ . Thus, Fig. 3 pictures the resultant function in real space if the modulus of the complex function is used. It is evident that these are cylindrically symmetrical distribution patterns in real space. It can be regarded as a requirement of cylindrical symmetry that the proper orbitals for a diatomic molecule also conform to the symmetry operations of a cylindrical point group (e.g.,  $D_{\infty h}$ ). This section illustrates the fact that proper superposition of  $\pi_g^{\ x}$  and  $\pi_g^{\ y}$  real orbitals to yield complex ones leaves no "lumpiness" of the real orbitals. The complex  $\pi$  orbital functions in fact have the appearance of figures of revolution of the real  $\pi$  orbital functions about the z axis. Matters are more complicated if we consider the effect of the inversion operator, î, on these complex orbitals because of the actual complex function behavior under coordinate interchange.

It is evident at face value that the real orbitals  $1\pi_g^x$  and  $1\pi_g^y$  (Fig. 3) for a diatomic molecule are gerade (even) under inversion, and also antibonding. We should also expect the complex orbitals  $1\pi_g^+$  and  $1\pi_g^-$  to be gerade (even) and antibonding. But the node in Fig. 3 for  $1\pi_e^+$  seems at first sight to be a contradiction. How can the node exist between the two atoms and still leave the  $1\pi_g^+$  gerade under i? Of course in the real orbital  $1\pi_{g}^{x}$  of Fig. 3 there are two nodes, allowing antibonding and gerade character to coexist. In the complex function  $1\pi_g^+$  depicted as a modulus figure in real space, the nodes are concealed in the complex character of the wave

13

function. (It will have occurred to the reader that the  $1\pi_g^x$  resembles the real atomic orbital  $3d_{xz}$  to which the molecular orbital should converge in the united-atom limit; and the  $1\pi_g^+$  resembles the complex atomic orbital  $3d_{+1}$ , to which in turn it should converge in the united-atom correlation.)

To test the behavior of  $1\pi_g^+$  under the inversion operator, î, we may write the orbital

$$1\pi_{e}^{+} = [Z'(z) - Z(z)] R(r) e^{i\phi}$$

in which the linear combination of atomic orbitals is resolved in z-coordinate components, since the  $\Phi(\phi)$  function is a common factor. Under the inversion operator,  $(z) \to (-z)$ ,  $(\phi) \to (\phi + \pi)$ , and r (a positive number) remains unchanged in cylindrical coordinates. Therefore

$$\hat{\mathbf{i}}(1\pi_{\mathbf{g}}^{+}) = [Z'(-z) - Z(-z)] R(r) e^{i\phi} e^{i\pi}$$

$$= (-1)[Z'(z) - Z(z)] R(r) e^{i\phi} (-1)$$

$$\hat{\mathbf{i}}(1\pi_{\mathbf{g}}^{+}) = (+1)(1\pi_{\mathbf{g}}^{+})$$

using  $e^{i\pi} = -1$ ; that is, the function is *gerade* (even). Thus, we cannot properly label the  $1\pi_g^+$  orbital regions of Fig. 3 as to sign since there is no way in which to illustrate on the modulus figure the effect of inversion on the complex functions.

## IV. THE MOLECULAR STATE FUNCTIONS FOR O2

#### A. The Molecular Orbital Configuration for Molecular Oxygen

We shall now proceed to build up a set of molecular state functions corresponding to the lowest energy molecular orbital configuration. R. S. Mulliken (1928, 1932) gave the first detailed spectroscopic description of the electronic states of the oxygen molecule shown in Fig. 1, following Lennard-Jones (1929) and Hückel (1930).

The most general molecular orbital configuration for molecular oxygen is given in Fig. 4 and the first line of Fig. 5. Each oxygen atom (Z=8) has the electron configuration  $1s^22s^22p^4$ . The inner atomic orbitals probably interact very weakly if at all, so that in most sources KK (atomic shells) is written to replace  $(1\sigma_g)^2(1\sigma_u)^2$ . The remaining twelve electrons may be considered to be the valency electrons, and according to the molecular orbital configuration, all of these are very busy acting in bonding or in antibonding roles. Thus, successively, there is a  $2\sigma_g$  bonding pair, followed in energy by

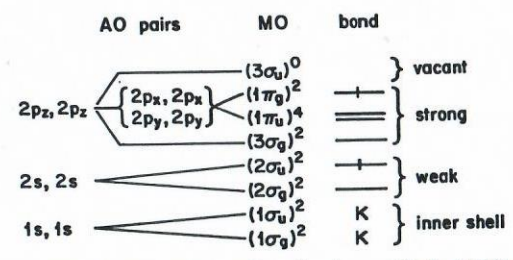


Fig. 4. Atomic orbital (AO) origin of molecular orbitals (MO) and bond type for homonuclear diatomic molecules.

a  $2\sigma_u$  antibonding pair; these probably correspond to weak interactions arising from the 2s atomic orbitals.

Next in order on the energy scale comes a  $3\sigma_{\rm g}$  bonding pair, in an orbital arising from the  $2p_{\rm z}$  orbitals on each atom, thus giving the oxygen its fundamental  $\sigma$  bond. This is followed by the doubly-degenerate  $1\pi_{\rm u}$  bonding orbital which is pictured in part in Fig. 3, top row  $(1\pi_{\rm u}^{\ x}$  and  $1\pi_{\rm u}^{\ y}$  being the real pair, and alternatively,  $1\pi_{\rm u}^{\ +}$  and  $1\pi_{\rm u}^{\ -}$  constitute the complex pair, discussed in the last section). Finally, there are two electrons in the  $1\pi_{\rm g}^{\ x}$ ,  $1\pi_{\rm g}^{\ y}$  (or  $1\pi_{\rm g}^{\ +}$ ,  $1\pi_{\rm g}^{\ -}$ ) antibonding orbital pictured in part in Fig. 3, bottom row. All but the last pair of orbitals are fully occupied and constitute closed shell contributions, so do not determine overall symmetry, angular momentum, or spin.

How the last pair of electrons in the abstract configuration ... $(1\pi_g)^2$  leads to six different electronic substates, in three classes, is the subject of this section. Thus, it is not accurate to state that the ground state of molecular oxygen is represented by the configuration shown in Fig. 4 and the top line of Fig. 5, since this identical configuration gives rise to three different electronic states with subcomponents.

A word on the "number of bonds" in ground state molecular oxygen would be instructive. If we designate electron-pair bonds by the traditional link —, and now electron-pair antibonds by +, we would arrive at the set of bonds shown in Fig. 4. Thus, the strong bonds holding the oxygen atoms together consist of one  $\sigma$ -bond and effectively one  $\pi$ -bond (the other  $\pi$ -bond is cancelled by the  $\pi$ -antibond; antibonding orbitals always more than cancel analogous bonding orbital effects). Thus, molecular oxygen in its ground state has two effective (net) electron-pair bonds, a picture entirely at variance with the Lewis structure representations of Fig. 2.

In particular we note that the two electrons in the  $\pi_g$  antibonding orbital effectively reduce the bonding strength of the four electrons in the  $\pi_u$  bonding orbitals, instead of being localized on atomic (essentially) nonbonding

sites. If we were to translate the molecular orbital bonding information given in Fig. 4 into a chemical formula for molecular oxygen, the clumsy but informative result would be\*

where the KK inner shell pairs are omitted since they are not valency electrons, and the "lone-pair" electrons shown are actually the weakly antibonding set  $(2\sigma_g)^2(2\sigma_u)^2$ . Because of the degeneracy of the  $\pi_g$  orbital, the above chemical formula corresponds to any of three different molecular states, which must now be examined.

# B. Spin and Orbital Angular Momenta for $\pi$ Orbital Assignments

Now we explore the building up of the proper molecular state functions. The configuration for  $O_2$  given in Fig. 4 and the top line of Fig. 5 is unrevealing because of the varieties of electron assignment of that last pair of electrons,  $1\pi_g^2$ . This is illustrated in the first column of Fig. 5. We choose the complex orbital set of Fig. 3 and the previous section, i.e.,  $\pi_g^+$  and  $\pi_g^-$ . Since electrons have spin, we must assign a spin wave function to each electron, either  $\alpha$  (spin-up) with  $+(1/2)(h/2\pi)$  units of spin angular momentum, or  $\beta$  (spin-down) with  $-(1/2)(h/2\pi)$  units of angular momentum. In column 1 of Fig. 5,  $\beta$  spin function is designated by a bar over the orbital symbol, and an  $\alpha$  spin function by an unbarred orbital symbol. For two electrons, with choices of + or - complex  $\pi$  orbital functions, and choices of  $\alpha$  or  $\beta$  spin, we arrive at an array of six possible resulting orbital assignments (column 1, Fig. 5).

To classify the orbital configuration components we identify their orbital angular momentum and spin angular momentum characteristics. We can do this by inspection, or by analytically testing each orbital configuration under orbital angular momentum and spin angular momentum operators for eigenvalues, using motion about the z axis as reference (the general symbol  $\hat{p}_{\phi}$  now being replaced by  $\hat{L}_z$  and  $\hat{S}_z$  for specific spectroscopic components). Inspection of  $\pi_g^+\pi_g^+$  indicates that  $+1(h/2\pi)$  plus  $+1(h/2\pi)$  units of orbital angular momentum (characteristic of  $\pi^+$ ) are involved), giving  $+2(h/2\pi)$  total units, corresponding to a  $\Delta$  state;  $\pi_g^+\pi_g^-$  indicates  $+1(h/2\pi)$  plus  $-1(h/2\pi)$  units of orbital angular momentum, or 0 total for

 $O_2 (|\sigma_g|^2 (|\sigma_u|^2 (2\sigma_g)^2 (2\sigma_u)^2 (3\sigma_g)^2 (|\pi_u|^4 (|\pi_g|^2$ 

1. Electronic Structure and Sensitization

ORBITAL SIGNMENT  $\widehat{Lz}$   $\widehat{Sz}$  COMPONENTS OF STATE  $\widehat{\pi_g}^+$   $\widehat{\pi_g}^+$  2 0  $\widehat{\Delta_g}$   $\widehat{\Delta_g}$   $\widehat{\pi_g}^+$   $\widehat{\pi_g}^-$  0 1  $\widehat{\Delta_g}$   $\widehat{\Delta_g}^ \widehat{\Delta_g}^ \widehat{\pi_g}^+$   $\widehat{\pi_g}^-$  0 0  $\widehat{\Delta_g}^ \widehat{\Delta_g}^ \widehat{\Delta_g$ 

Fig. 5. Molecular oxygen configuration components.

a  $\Sigma$  state; and e.g.,  $\pi_g^-\pi_g^-$  indicates that  $-1(h/2\pi)$  plus  $-1(h/2\pi)$ , or  $-2(h/2\pi)$  total units, corresponding again to a  $\Delta$  state (total orbital angular momentum units  $0, 1, 2, 3, \ldots, (h/2\pi)$  corresponding to  $\Sigma, \prod, \Delta, \Phi \ldots$  states).

The spin angular momentum components are also discernible on inspection for the orbital configuration assignments of column 1, Fig. 5. The assignment  $\pi_g^+\bar{\pi}_g^+$  indicates spin functions successively for the two electrons as  $\alpha\beta$  or  $+(1/2)(h/2\pi)$  plus  $-(1/2)(h/2\pi)$  units, a net of 0 units of spin angular momentum, thus a singlet state component,  ${}^1\Delta_g$ ;  $\pi_g^+\pi_g^-$  indicates spin functions  $\alpha\alpha$ ,  $+(1/2)(h/2\pi)$  plus  $+(1/2)(h/2\pi)=1(h/2\pi)$  net units of spin angular momentum, thus a triplet state component,  ${}^3\Sigma_g^-$ . Rather unfamiliarly for chemists, orbital assignments like  $\pi_g^+\bar{\pi}_g^-$ , with spin function  $\alpha\beta$ , and  $\bar{\pi}_g^+\pi_g^-$  with spin function  $\beta\alpha$ , therefore spin-component  $M_S=0$ , can be singlet state components or a triplet state (zero spin) component, since  $\alpha\beta-\beta\alpha$ , and  $\alpha\beta+\beta\alpha$  must later be formulated for the complete spin functions (see below).

Thus, the two  ${}^1\Delta_g$  states are unambiguously or uniquely designated by the simple orbital configuration assignment; the  $M_S=+1$  and  $M_S=-1$  components of the  ${}^3\Sigma_g^-$  state are also uniquely designated. The configuration for the  ${}^1\Sigma_g^+$  state and the  ${}^3\Sigma_g^-$  ( $M_S=0$ ) state must be resolved by taking linear combinations of the equivalent orbital assignments  $\pi_g^+\bar{\pi}_g^-$  and  $\bar{\pi}_g^+\pi_g^-$ . The test of whether the linear combination is really  ${}^3\Sigma_g^-$  ( $M_S=0$ ) or  ${}^1\Sigma_g^+$  can be accomplished by factoring out the spin functions from the completed wave function, or by testing with the total spin angular momentum operator  $S^2$  (distinguishing triplets from singlets).

<sup>\*</sup> This formula is exactly analogous to Pauling's three-electron bond structure for oxygen (Pauling, 1960), where we perceive that the two extra electrons of the two three-electron bonds must be in the antibonding orbital.

Biri.

# C. Construction of Determinantal Wave Functions for $\pi$ Electron States of $O_2$

The properties of an electron indicate that it behaves like a fermion, that is, it conforms to a Fermi-Dirac statistical distribution. Concomitant with this behavior is the requirement of an antisymmetric total wave function, i.e., one that changes sign upon electron interchange. It is convenient to express proper electron wave functions therefore in determinantal form (Slater determinant), since interchanging any two rows or columns of a determinant intrinsically changes its net sign, and such an interchange corresponds to interchange of electron numbering.

Determinantal wave functions for molecular oxygen based on complex orbital functions are tabulated in Fig. 6. For simplification, the g subscript has been dropped in this formulation, since all of the orbitals involved are the  $\pi_g$  orbitals, and the +, - superscripts have become subscripts. It is customary to simplify the writing of these determinants by writing only the principal diagonal. Thus for one of the  ${}^1\Delta_g$  states

$$\Psi(^{1}\Delta_{g}) = \frac{1}{\sqrt{2}} |\pi_{+}\bar{\pi}_{+}| = \frac{1}{\sqrt{2}} |\pi_{+}(1)\alpha(1) \cdots \pi_{+}(2)\beta(2)|$$

wherein the two-electron orbital assignment of column 1, Fig. 5 corresponds

STATE	COMPLEX WAVE FUNCTION $\frac{1}{2} \left\{  \pi_{+} \ \overline{\pi}_{-}  -  \overline{\pi}_{+} \ \pi_{-}  \right\}$	SPIN-ORBITAL DIAGRAM
<b>¹</b> ∆ <sub>g</sub>	$\begin{bmatrix} \frac{1}{\sqrt{2}} &   \pi_{+} \ \overline{\pi}_{+} \   \\ \frac{1}{\sqrt{2}} &   \pi_{-} \ \overline{\pi}_{-} \   \end{bmatrix}$	
$^{3}\Sigma_{g}^{-}$	$\begin{cases} \frac{1}{\sqrt{2}} &  \pi_{+} \pi_{-}  \\ \frac{1}{2} \left\{  \pi_{+} \overline{\pi}_{-}  +  \overline{\pi}_{+} \pi_{-}  \right\} \\ \frac{1}{\sqrt{2}} &  \overline{\pi}_{+} \overline{\pi}_{-}  \end{cases}$	

Fig. 6. Complex wave functions for the lowest electronic states of molecular oxygen.

to the product obtained from the principal diagonal; the full determinant is then

$$\Psi(^{1}\Delta_{g}) = \frac{1}{\sqrt{2}} \begin{vmatrix} \pi_{+}(1)\alpha(1) & \pi_{+}(2)\alpha(2) \\ \pi_{+}(1)\beta(1) & \pi_{+}(2)\beta(2) \end{vmatrix}$$

This determinant may be expanded to yield

$$\Psi(^{1}\Delta_{g}) = \frac{1}{\sqrt{2}} \left[ \pi_{+}(1)\alpha(1)\pi_{+}(2)\beta(2) - \pi_{+}(1)\beta(1)\pi_{+}(2)\alpha(2) \right]$$

Thus, in the determinant, columns label electrons 1 and 2, rows label orbital assignment  $\pi_{+}\alpha$  and  $\pi_{+}\beta$ . For the determinantal form of the state wave function and in the expanded form of the wave function, it is evident that (a) interchange of 1 and 2 changes the sign of the overall wave function, as required for all proper (antisymmetrized) wave functions and (b) indistinguishability of electrons is now implicit in the formulation. The expanded expression can be factored into orbital and spin parts

$$\Psi(^{1}\Delta_{g}) = \frac{1}{\sqrt{2}} \left[ \pi_{+}(1)\pi_{+}(2) \right] \left[ \alpha(1)\beta(2) - \beta(1)\alpha(2) \right]$$

where the spin function is clearly the antisymmetric two-electron spin function, i.e., singlet; and the orbital function is symmetric under electron interchange (for a net antisymmetry as required).

Using the linear combination of  $(\pi_g^+\bar{\pi}_g^- - \bar{\pi}_g^+\pi_g^-)$  of Fig. 5, column 1, written in determinantal form for electron indistinguishability, we obtain the unique wave function for the  ${}^1\Sigma_g^+$  state

$$\Psi(^{1}\Sigma_{g}^{+}) = \frac{1}{2}(|\pi_{+}\bar{\pi}_{-}| - |\bar{\pi}_{+}\pi_{-}|)$$

which factors after expansion of the determinants into

$$\Psi(^{1}\Sigma_{\sigma}^{+}) = \frac{1}{2} \{ \lceil \pi_{+}(1)\pi_{-}(2) \rceil + \lceil \pi_{-}(1)\pi_{+}(2) \rceil \} \lceil \alpha(1)\beta(2) - \beta(1)\alpha(2) \rceil$$

again revealing a singlet spin function, with a symmetric orbital function under electron interchange.

Finally, as a last example we resolve the  ${}^3\Sigma_g^ (M_S=0)$  component, for which Fig. 6 indicates the determinantal form of the linear combination  $(\pi_g^+\bar{\pi}_g^- + \bar{\pi}_g^+\pi_g^-)$  of Fig. 5, column 1

$$\Psi(^{3}\Sigma_{g}^{-}, M_{S} = 0) = \frac{1}{2}(|\pi_{+}\bar{\pi}_{-}| + |\bar{\pi}_{+}\pi_{-}|)$$

which factors upon expansion of the determinants into

$$\Psi(^{3}\Sigma_{\sigma}^{-}, M_{S} = 0) = \frac{1}{2} \{ [\pi_{+}(1)\pi_{-}(2)] - [\pi_{-}(1)\pi_{+}(2)] \} [\alpha(1)\beta(2) + \beta(1)\alpha(2)] \}$$

revealing a symmetric or triplet spin function and an antisymmetric orbital function, under electron interchange. This last represents an electronic state with zero component of spin angular momentum with respect to the z axis. The remaining state functions of Fig. 6 are formulated analogously from the components of Fig. 5, column 1.

Thus, the compactness of the determinantal form as displayed in Fig. 6 for the lowest electronic states of molecular oxygen permits a full resolution into electronic state components and at the same time reveals their distinctive differences as well as features in common. We may summarize as follows.

From the single molecular orbital configuration ...  $(1\pi_g)^2$  we have generated six different electronic states with distinctive electronic distribution patterns, energies, and magnetic characteristics. There is a unique  $^1\Sigma_g^+$  state; there are in zeroth approximation two equal energy  $^1\Delta_g$  states and three equal energy  $^3\Sigma_g^-$  states. Arising as they do from a single molecular orbital configuration, we could anticipate the potential curve (Fig. 1) common features for the cluster of  $^1\Sigma_g^+$ ,  $^1\Delta_g$ , and  $^3\Sigma_g^-$  states: they have nearly coincident potential minima, indicating almost identical binding energies, and the states dissociate to a common limit.

# D. Electron Repulsion in the $\pi$ Electron States of $O_2$

The relative energy of the lowest molecular oxygen states was first discussed by Hückel (1930) in his paper: "Quantum Theory of the Double Bond." All of the states described by the wave functions of Fig. 6 would be degenerate in the absence of electron-electron interaction. Electron repulsion splits the states apart in energy, and Hückel showed that the energy of the  ${}^{1}\Delta_{g}$  state should be approximately half of the sum of the energies of the  $^1\Sigma_g^{}^-$  and the  $^3\Sigma_g^{}^-$  states. The argument presented by Hückel is so elegant, revealing, and simple that it is worth presenting here, especially since it has escaped the attention it deserves. The idea is based essentially on correlation of motion of the two electrons in the  $\pi_{\rm g}$  orbital with respect to the cylindrical axial angle  $\phi$ . We may demonstrate Hückel's argument by starting with the spin-factored two-electron state functions just presented in Fig. 6. Factoring out the Z(z) and R(r) parts, and substituting the  $\Phi(\phi)$ part of the function for the  $\pi$  orbitals using  $\Phi(\phi) = (1/\sqrt{2\pi})e^{im_l\phi}$  with  $m_l = +1$ for  $\pi_+$  and -1 for  $\pi_-$ , we obtain the  $\phi$ -dependence of the orbital part of the state functions  $\psi$  (primed)

$$\begin{split} \Psi'(^{1}\Sigma_{\mathbf{g}}{}^{+}) &= \frac{1}{2}\{[\pi_{+}(1)\pi_{-}(1)] + [\pi_{-}(1)\pi_{+}(2)]\} \\ &= \frac{1}{4\pi}(e^{i\phi_{1}}e^{-i\phi_{2}} + e^{-i\phi_{1}}e^{i\phi_{2}}) \\ &= \frac{1}{4\pi}(e^{i(\phi_{1}-\phi_{2})} + e^{-i(\phi_{1}-\phi_{2})}) \\ \Psi'(^{1}\Delta_{\mathbf{g}}) &= \frac{\sqrt{2}}{4\pi}[\pi_{+}(1)\pi_{+}(2)] = \frac{\sqrt{2}}{4\pi}[e^{i\phi_{1}}e^{i\phi_{2}}] \\ &= \frac{\sqrt{2}}{4\pi}e^{i(\phi_{1}+\phi_{2})} \\ \Psi'(^{1}\Delta_{\mathbf{g}}) &= \frac{\sqrt{2}}{4\pi}[\pi_{-}(1)\pi_{-}(2)] = \frac{\sqrt{2}}{4\pi}[e^{-i\phi_{1}}e^{-i\phi_{2}}] = \frac{\sqrt{2}}{4\pi}e^{-i(\phi_{1}+\phi_{2})} \\ \Psi'(^{3}\Sigma_{\mathbf{g}}{}^{-})_{0} &= \frac{1}{2}\{[\pi_{+}(1)\pi_{-}(2)] - [\pi_{-}(1)\pi_{+}(2)]\} \\ &= \frac{1}{4\pi}(e^{i\phi_{1}}e^{-i\phi_{2}} - e^{-i\phi_{1}}e^{i\phi_{2}}) \\ &= \frac{1}{4\pi}(e^{i(\phi_{1}-\phi_{2})} - e^{-i(\phi_{1}-\phi_{2})}) \end{split}$$

1. Electronic ructure and Sensitization

so that for the  $\Phi(\phi)$  parts of the orbital two-electron state functions

$$\Psi'(^{1}\Sigma_{g}^{+}) = \frac{1}{2\pi}\cos(\phi_{1} - \phi_{2})$$

$$\Psi'(^{1}\Delta_{g}) = \frac{\sqrt{2}}{4\pi}e^{i(\phi_{1} + \phi_{2})}$$

$$\Psi'(^{1}\Delta_{g}) = \frac{\sqrt{2}}{4\pi}e^{-i(\phi_{1} + \phi_{2})}$$

$$\Psi'(^{3}\Sigma_{g}^{-})_{0} = \frac{1}{2\pi}\sin(\phi_{1} - \phi_{2})$$

These two electron state functions show the dependence on the difference in angular position  $\phi$  for the two  $\pi_g$  electrons in each state. The square (or complex modulus) of these wave functions corresponds to electron probability or point density. Since electron-electron repulsion is determined by the operator  $e^2/r_{12}$ , there is a great sensitivity of repulsive interaction to closeness of approach. The  $\Psi(^1\Sigma_g^+)$  state shows a cosine squared dependence of the  $(\phi_1-\phi_2)$  angular difference (Fig. 7) for the probability density  $(\Psi^*\Psi)$  for the two electrons, i.e., they tend to maximize (cos 0=1) probability density for zero angular difference: the electron repulsion interaction will be a maximum. The  $\Psi(^3\Sigma_g^-)_0$  state shows a sine squared dependence of the  $(\phi_1-\phi_2)$  angular difference (Fig. 7) for a maximum probability density  $(\Psi^*\Psi)$  for 90° angular difference (sin 90° = 1): the electrons avoid each other, and the electron repulsion interaction will be a minimum for the

 $y^{1}$   $y^{2}$   $y^{3}$   $y^{3}$   $y^{4}$   $y^{4}$   $y^{4}$   $y^{4}$   $y^{4}$   $y^{4}$   $y^{4}$   $y^{4}$   $y^{4}$   $y^{4}$ 

Fig. 7. Angular correlation for the two valency electrons in the lowest states of molecular oxygen.

triplet state. This is a well-known intuitive result, but Hückel's argument has the additional feature of an angular correlation analysis. The  $\Psi(^1\Delta_{\rm g})$  state functions yield complex modulus  $|\Psi^*\Psi|=1$  so that the two electrons have an electron repulsion averaged over the entire orbital. Hückel (1930) used simple product orbitals for the two-electron functions. We have shown that his argument holds perfectly well for determinantal functions. Hückel then demonstrated by simple comparison of electron repulsion integrals that

$$E(^{1}\Delta) = (1/2)[E(^{1}\Sigma) + E(^{3}\Sigma)]$$

to first approximation.

A comment might be added on the consequence of the electron repulsion argument for triplet state lowering of energy versus singlet state raising of energy from a common or degenerate configuration. This is, of course, Hund's rule: the state of maximum multiplicity for a given configuration lies lowest. The role of spin in the Hückel argument is indirect: the antisymmetric and symmetric spin functions constrain the corresponding *orbital* occupancies to be, respectively, symmetric and antisymmetric; it is the form of the *orbital function* which then leads to cosine and sine dependence of angular correlation for singlet and triplet electron pairs.

# E. Degeneracies in the $\pi$ Electron States of $O_2$

Electron cell diagrams are given on the right side of Fig. 6 to offer some graphical comparisons of the various electron distributions corresponding to the different lowest electronic state components. The diagrams correspond exactly to the principal diagonal terms of the determinants. Thus,

electron exchange is not shown in the cell diagrams because, as seen earlier, indexing of orbital occupation is given by the alternate diagonal product of the determinant. It is also clear from the cell diagrams that each state component has a qualitatively different arrangement of electrons, orbitals, and spins. The origin of the  $^1\Delta_g$  state degeneracy stands out clearly. The  $^1\Sigma_g^+$  state cell diagram has some apparent resemblance to that for the  $^3\Sigma_g^ (M_S=0)$  state, except for the sign of the linear combination of the determinants. Of course, the difference is crucial: when investigating electron probability density, the cross term or interference term appears with opposite sign.

The triplet state degeneracy can bear a little elaboration. We have already shown using the Hückel argument that

$$\Psi'(^{3}\Sigma_{g}^{-})_{(M_{S}=0)} = \frac{1}{2\pi}\sin(\phi_{1} - \phi_{2})$$

leading to minimization of electron repulsion by angular correlation. The  $\phi$  part of the orbital state wave function was given as

$$\Psi'(^{3}\Sigma_{\mathbf{g}}^{-})_{(M_{S}=0)} = \frac{1}{2} \{ [\pi_{+}(1)\pi_{-}(2)] - [\pi_{-}(1)\pi_{+}(2)] \}_{\text{orb.}}$$

The determinantal forms of the state functions for the  $M_{\rm S}=+1$  and -1 triplet components are quite different in form (Fig. 6) from that for the  $M_{\rm S}=0$  triplet component. If we expand the determinants, factor out the spin functions, and regroup the terms, we obtain for the  $\Phi(\phi)$  part of the orbital state functions

$$\begin{split} &\Psi'(^{3}\Sigma_{g}^{-})_{(M_{S}=1)} = \frac{1}{2}\{\left[\pi_{+}(1)\pi_{-}(2)\right] - \left[\pi_{-}(1)\pi_{+}(2)\right]\}_{\text{orb.}} \\ &\Psi'(^{3}\Sigma_{g}^{-})_{(M_{S}=-1)} = \frac{1}{2}\{\left[\pi_{+}(1)\pi_{-}(2)\right] - \left[\pi_{-}(1)\pi_{+}(2)\right]\}_{\text{orb.}} \end{split}$$

Thus, all of the orbital components of the three  ${}^3\Sigma_g^-$  state components are identical and will have the same  $\sin(\phi_1 - \phi_2)$  dependence (Fig. 7), with the same angular avoidance of electron repulsion. In other words, the three symmetric spin functions, even though differing from each other, constrain the orbital part of the triplet state components to be antisymmetric and identical, with energy identity (degeneracy).

It is interesting to point out that, at least in the free oxygen molecule, although the critical pair of electrons avoid each other, the correlation of motion is angle to angle, rather than end to end as in the primitive chemical picture for a triplet state. The other aspect which bears elaboration for the three triplet state components is the relation of the projection of spin angular momentum onto the z axis (the eigenvalues of the  $S_z$  operator) to the total spin for each component (the eigenvalues of the  $S_z$  operator). The quantum

1. Electr

numbers  $M_{\rm S}=+1$ , 0, and -1 each correspond to eigenvalues of the  $\widehat{S}_{\rm z}$  operator; they are successively the z components of spin angular momentum (in units  $h/2\pi$ ). The total spin is given by the  $\widehat{S}^2=S_{\rm z}^{\ 2}+S_{\rm y}^{\ 2}+S_{\rm x}^{\ 2}$  operator, with eigenvalues  $S(S+1)h^2/4\pi^2$ . For each of the triplet state components the total spin quantum number S is 1; as triplet states, each component does have the same net spin. In this regard, the  $^1\Sigma_{\rm g}^{\ +}$  state differs from the  $^3\Sigma_{\rm g}^{\ -}$  ( $M_{\rm S}=0$ ) component; for the singlet state, although  $M_{\rm S}=0$ , also S=0, with zero net spin angular momentum.

#### F. The Real $\pi$ Electron State Functions for $O_2$

Real state functions for molecular oxygen are presented in Fig. 8 for the three lowest states under discussion. A comparison of the determinantal form for these and for the complex state functions of Fig. 6 indicates an interesting juggling of terms and signs. The procedure for converting the complex forms is straightforward, and like the process of expanding the determinants and factoring out the spin functions summarized earlier, the reader will find it of interest to work out these conversions. The procedure is: (a) expand the determinants given in Fig. 6 into differences of products, with electron index labeling as exemplified earlier in this section; (b) substitute  $\pi_+$  by  $(1/\sqrt{2})(\pi_x + i\pi_y)$  and  $\pi_-$  by  $(1/\sqrt{2})(\pi_x - i\pi_y)$ ; (c) cancel common terms, and regroup into new determinantal products; (d) condense to the

STATE	REAL WAVE FUNCTION	SPIN-ORBITAL DIAGRAM
$^{1}\Sigma_{\mathbf{g}}^{\mathbf{+}}$	$\frac{1}{2}\left\{ \mid \pi_{x} \; \overline{\pi}_{x} \mid + \mid \pi_{y} \; \overline{\pi}_{y} \mid \right\}$	$[ \bigoplus_{x} \bigcirc_{y}] + [ \bigcirc_{x} \bigoplus_{y}]$
	L	$ \begin{bmatrix} \bigoplus_{x} \bigcirc_{y} \end{bmatrix} - \begin{bmatrix} \bigcirc_{x} \bigoplus_{y} \end{bmatrix} $ $ \begin{bmatrix} \bigoplus_{x} \bigoplus_{y} \end{bmatrix} - \begin{bmatrix} \bigoplus_{x} \bigoplus_{y} \end{bmatrix} $
$^3\Sigma_{\mathfrak{g}}^-$	$\begin{bmatrix} \frac{1}{\sqrt{2}} &  \pi_{x} \pi_{y}  \\ \frac{1}{2} \left\{  \pi_{x} \overline{\pi}_{y}  +  \overline{\pi}_{x} \pi_{y}  \right\} \\ \frac{1}{\sqrt{2}} &  \overline{\pi}_{x} \overline{\pi}_{y}  \end{bmatrix}$	

Fig. 8. Real wave functions for the lowest electronic states of molecular oxygen.

determinantal diagonal abbreviated form. The behavior of each transformation varies. For  ${}^{1}\Sigma_{g}^{+}$ , all imaginary terms cancel. For  ${}^{3}\Sigma_{g}^{-}$  ( $M_{S}=+1$ ) and  $M_{S}=-1$  transformation, all real terms cancel; the common coefficient i for remaining terms is merely a phase factor and is eliminated by multiplying by -i. For the  ${}^{1}\Delta_{g}$  transformations, one yields an expression in the form A+iB and the other in the form A-iB. Since the goal is to obtain a real set of determinantal state functions, addition and subtraction yield 2A and 2iB, which are simply renormalized and then appear as shown in Fig. 8.

The real state functions of Fig. 8 now confirm neatly what we learned about angular correlation for the  ${}^{1}\Sigma_{g}{}^{+}$  and  ${}^{3}\Sigma_{g}{}^{-}$  states. Each of the terms of  ${}^{1}\Sigma_{g}{}^{+}$  is of the form  $\pi_{x}\pi_{x}$  or  $\pi_{y}\pi_{y}$ , confirming the Fig. 7 correlation of electron pairs forced to move most probably in a common plane, with  $\phi_{1}-\phi_{2}$  a minimum. Each of the terms for the  ${}^{3}\Sigma_{g}{}^{-}$  state components is of form  $\pi_{x}\pi_{y}$ , indicating that each electron of the pair moves most probably in perpendicular planes, minimizing repulsion with  $\phi_{1}-\phi_{2}$  equal to 90° as shown in Fig. 7. The  ${}^{1}\Delta_{g}$  states represent xx, yy two-electron terms and also xy, xy terms: taken together, this degenerate pair of states averages the energy for the  ${}^{1}\Sigma_{g}{}^{+}$  and the  ${}^{3}\Sigma_{g}{}^{-}$  states, in the free molecule.

However, if a perturbing field is applied by an approaching molecule, the  ${}^{1}\Delta_{g}$  state degeneracy will split. In such a case, xz (and yz) planes are defined by an approaching molecule. Thus, one could begin to elucidate reaction mechanisms on the basis of electron distribution in the real  $\pi$  orbital wave functions of the oxygen molecule. For example, the  ${}^{1}\Sigma_{g}^{+}$  state would tend to have both of the  $\pi$  electrons in plane, so that concerted two-point addition reactions could be visualized (with the added step of polarization of the  $\pi$  electrons onto the atomic centers). The  ${}^{3}\Sigma_{g}^{-}$  state(s) would tend to have each of the  $\pi$  electrons oriented in mutually perpendicular planes, so an intermediate with single point attachment might be anticipated. The  ${}^{1}\Delta_{g}$  state, however, under perturbation by an approaching molecule in one plane would tend to show a distribution of products reflecting both concerted two-point addition and single-point attachment intermediates.

# G. The Literature on Molecular Oxygen Structure

We have indulged in a somewhat detailed examination of the electronic structure of molecular oxygen in its three lowest states because of the absence of specific information in standard sources. Three classic reference works [Pauling and Wilson (1935); Eyring, Walter, and Kimball (1944); Kauzmann (1957)] fail to include oxygen in the index of the book. Under diatomic molecules, the last two references give the level of treatment corre-

sponding to Fig. 4 with *ad hoc* state symbols, which is about the level of treatment of electronic structure of oxygen given in most contemporary valency theory and quantum theory books today.

Ballhausen and Gray (1964) presented an unlabeled set of state wave functions corresponding to those of Fig. 8, although the given atomic orbital composition indicates the functions to be real. Griffith (1964a,b) presented a set of real state wave functions for oxygen, with diverse forms of spin factoring. Kearns (1971) presented a set of complex state functions for oxygen, giving only the  $M_{\rm S}=0$  component of the triplet. He also gave a corresponding set of real state functions. The normalization constants are inconsistent in the sources mentioned above; the present set agrees with those of Griffith. Kasha and Khan (1970) presented a complete set of state wave functions for molecular oxygen, unfortunately with an error in labeling: their Fig. 8 labels the orbitals as complex, whereas the form of the functions shows that they are the real set. Therefore, their Fig. 8 should have subscripts + and - replaced by x and y respectively, to agree with Fig. 8 of the present chapter.

Quantum mechanical calculations on the lowest electronic states of the oxygen molecule have been given by Moffitt (1951), Meckler (1953), and Kotani et al. (1957).

# V. SENSITIZATION MECHANISMS FOR SINGLET OXYGEN

The experimental energy level diagram for the electronic transitions involving the lowest three electronic states of molecular oxygen (Fig. 9) is now firmly established by experimental and theoretical researches. The single molecule transitions (Fig. 1)  $^1\Delta_g \leftarrow {}^3\Sigma_g^-$  and  $^1\Sigma_g^+ \leftarrow {}^3\Sigma_g^-$  have been known as classical atmospheric absorption bands at low sun (Herzberg, 1950). These lowest two transitions are strictly forbidden for electric dipole radiation in the isolated molecule, and result in extraordinary metastability of the excited singlet states of oxygen. The lifetimes estimated by integrated absorption measurements are 45 min for the  $^1\Delta_g$  state, and 7.1 sec for the  $^{1}\Sigma_{g}^{+}$  state at zero pressure, but even at 1 atm pressure intermolecular collisions change the transition mechanism to electric dipole, with much shortened lifetimes. Figure 9 indicates intermolecular collision pairs with ground state molecular oxygen for the three lowest oxygen states, e.g.,  $(^{1}\Delta_{g})[^{3}\Sigma_{g}^{-}]$ , as a mechanism for electronic relaxation of the multiplicity selection rule. The lifetimes in solution for the singlet molecular oxygen states become drastically shortened, with estimates of  $10^{-3}$  sec for the  $^{1}\Delta_{g}$ state and  $10^{-9}$  sec for the  $^1\Sigma_g^+$  state in water (Arnold et al., 1968). The life-

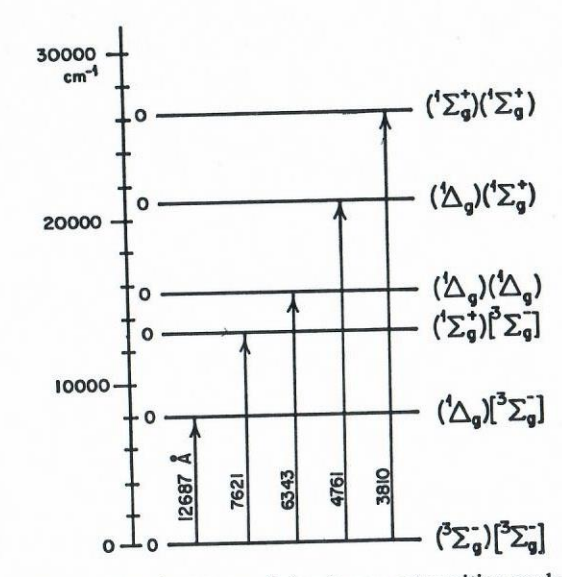


Fig. 9. Oxygen single molecule states and simultaneous transition molecular-pair states.

times of the  $^1\Delta_g$  state of oxygen have been measured (Merkel and Kearns, 1972; Long and Kearns, 1975) to be in the range  $10^{-6}$ – $10^{-3}$  sec, with a strong solvent dependence. The first definitive observations on the  $^1\Delta_g$  state were made by the Herzbergs (1934, 1947, 1948) after observation of this state in liquid oxygen absorption by Ellis and Kneser (1933).

Singlet molecular oxygen became a subject of intense laboratory study as a chemical reagent following the interpretation by Khan and Kasha (1963) of the chemiluminescence of the hypochlorite-oxygen reaction as due to liberated singlet oxygen. The complicated history of rediscoveries and reinterpretation has been carefully traced (Kasha and Khan, 1970; Khan and Kasha, 1970; Kearns, 1971). An indication of the vast attention that singlet oxygen is now receiving is given by the publication of a reprint volume summarizing the chemical history of this subject (Schaap, 1976).

The clue to spectroscopic and photochemical behavior of singlet oxygen excited states lies in understanding the simultaneous transitions which are possible for collision pairs of singlet oxygen molecules. The idea originated with Ellis and Kneser (1933), who sought to explain the blue color and absorption spectrum details of liquid oxygen on the basis of molecular-pair absorption. They were influenced by G. N. Lewis' concept of  $(O_2)_2$  dimers as an explanation of the paramagnetic behavior of liquid oxygen diluted by liquid nitrogen. All subsequent research has indicated definitively that no dimers of molecular oxygen exist at ordinary conditions, and that the

and Dale E. Brabham

intermolecular perturbations, necessary to account for the collisional enhancement of the single-molecule transitions and the simultaneous transitions, are much smaller than kT. The term "dimol" which is commonly applied to singlet-molecular oxygen pairs is thus devoid of operational meaning and should not be used (Kearns, 1971; cf. Krupenie, 1972, esp. pp. 440-443; cf. Gray and Ogryzlo, 1969). Dimers of molecular oxygen are found in solid oxygen at very low temperatures.

Chemiluminescence observations of the hypochlorite-peroxide reaction were related to simultaneous transitions in molecular pairs by a series of investigators (Groh and Kirrmann, 1942; Stauff and Schmidkunz, 1962; Arnold et al., 1964; cf. Khan and Kasha, 1970), but it was the work of Ogryzlo's laboratory (Arnold et al., 1964; Browne and Ogryzlo, 1964) which related the observed chemiluminescence spectra of the hypochlorite-solution reaction to the electrical discharge molecular oxygen spectra in the vapor phase. Subsequently, Khan and Kasha (1970) gave a full spectroscopic correlation of absorption and emission spectra corresponding to simultaneous transition states shown in Fig. 9 for molecular pairs.

We may define the simultaneous transition as a transition for a pair of atomic or molecular species to a composite excited state (a one-photon twomolecule cooperative absorption), the energy of the new state arising by a nonresonance, superposition of two excited state energies of the component species; the converse simultaneous process may take place with the emission of a photon. We may neglect the shift of the new state relative to the sums of the component state energies on the basis of the very small interaction. The phenomenon of simultaneous transition is very widely observed in infrared spectroscopy and especially in electronic spectroscopy of forbidden transitions. The latter make the simultaneous transition easy to observe, both by the enhancement effects found, as well as by the natural "spectral window" they afford. In the case of singlet molecular oxygen, we may perceive a molecular pair state  $({}^{1}\Delta_{\circ})({}^{1}\Delta_{\circ})$  as giving rise to a unique singlet multiplicity, S, whereas the ground state pair  $({}^{3}\Sigma_{\alpha}^{-})({}^{3}\Sigma_{\alpha}^{-})$  would give rise to S + T + Q multiplicity, permitting the multiplicity allowed singlet  $\rightarrow$ singlet transition to occur.

The simultaneous transition for a pair of absorbing or emitting species does not require an actual "complex" to exist, but the two molecules (atoms, ions) must be within electron exchange "contact". In condensed phases, such as liquid oxygen, enough collision pairs exist for a weak but finite absorption to be observed. In the gas phase, 10 cm optical paths and oxygen pressures in excess of 100 atm are needed (cf. Khan and Kasha, 1970) to observe the simultaneous transition in absorption. In emission with singlet oxygen pairs, even at pressures below 1 atm, the simultaneous transition is readily observed. Blowing Cl2 gas via a sintered glass filter into alkaline 15% H<sub>2</sub>O<sub>2</sub>, 1 M in OH<sup>-</sup>, yields red emission easily seen in a half-darkened room [the  $(^1\Delta_g)(^1\Delta_g) \rightarrow (^3\Sigma_g^{-})(^3\Sigma_g^{-})$  emission]. Obviously, the metastability of  ${}^{1}\Delta_{g}$ , even at 1 atm, is still great enough to permit two excited molecules to collide and produce a simultaneous transition state.

Sensitization mechanisms involving singlet molecular oxygen are of great chemical and biological importance. Khan and Kasha (1966) proposed that some organic molecule "chemiluminescences" could be the result of excitation by a physical energy transfer from singlet oxygen simultaneous transition states, such as the  $(^1\Delta_g)(^1\Delta_g)$  state, or the  $(^1\Sigma_g^{\ +})(^1\Delta_g)$  state. The theory of such processes has been elaborated on in two papers from Kearns' laboratory (Kawaoka et al., 1967; Khan and Kearns, 1968). We have been exploring energy resonances between the simultaneous transition states for singlet molecular oxygen (Fig. 9) and various dye molecules stable in the peroxide-hypochlorite reaction system. Here we shall review five possible mechanisms for such physical energy transfer excitation processes for the dye "chemiluminescences".

# Mechanism a: Triplet Energy Pooling

A chemiluminescence mechanism suggested by Ogryzlo and Pearson (1968) and investigated by Wilson (1969) for rubrene and violanthrone is given in Fig. 10. This energy pooling mechanism requires two successive energy transfer excitations by a  ${}^{1}\Delta_{g}$  state, first lifting the dye molecule to its lowest triplet.state, then this triplet state being further promoted to or above its lowest singlet excited state. The energetic criteria are

$$\Delta E_{\mathrm{S}_{1}} < 2(\Delta E_{\mathrm{1}_{\Delta_{\mathbf{g}}}})$$
 $\Delta E_{\mathrm{T}_{1}} < \Delta E_{\mathrm{1}_{\Delta_{\mathbf{g}}}}$ 

Molecules which have as low an energy for the lowest triplet state as is required by the energy pooling mechanism of Ogryzlo and Pearson are rare.

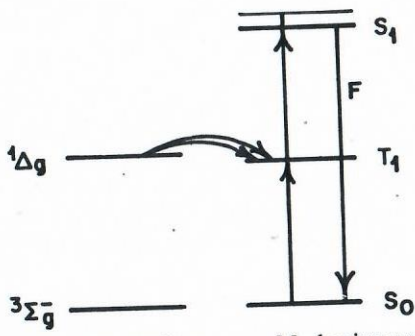


Fig. 10. Photosensitization by singlet oxygen. Mechanism a: Molecular triplet energy pooling.

Moreover, generally in dyes, singlet-triplet separations diminish as the lowest excited singlet state energy decreases (and molecular size increases). It is true that in aromatic hydrocarbons singlet-triplet splits can get as large as 12000 cm<sup>-1</sup>. In the case of rubrene and also violanthrone, the lowest triplet state has not yet been located experimentally. We conclude that if the energy pooling mechanism is valid, it will apply to very few cases.

# Mechanism b: Double-Molecule Sensitization

This is a form of the physical sensitization mechanism proposed by Khan and Kasha (1966). The possible criteria for the various simultaneous transition or double-molecule state (Fig. 9) are (cf. Fig. 11)

Fig. 11. Photosensitization by singlet oxygen. Mechanism b: Sensitization by simultaneous transition state.

We believe that this mechanism may apply to many red-luminescing dyes which satisfy the first energy criterion. As is commonly known, the  ${}^{1}\Delta_{g}$  state seems to be the one predominantly produced in the hypochlorite-peroxide reaction, so the chance of  $({}^{1}\Delta_{g})({}^{1}\Delta_{g})$  collision pairs existing is greatest, compared with the other two cases. It is impressive that the relative quantum yield of singlet-oxygen-sensitized dye luminescence is always much greater than the quantum yield of the oxygen simultaneous state direct emission. When the  $O_2$ - $O_2$  emission is observed, it is only from those molecules which have eluded quenching in the aqueous phase and escaped into the bubbles (Khan and Kasha, 1964), from which the characteristic red

glow of  $({}^{1}\Delta_{g})({}^{1}\Delta_{g})$  emission is seen. Obviously, energy transfer from molecular oxygen pairs to the acceptor molecule competes favorably in rate with the quenching. We believe the violanthrone and rubrene cases may prove to fit this present mechanism.

## Mechanism c: Delayed Fluorescence Sensitization

1. Electronic Lucture and Sensitization

The case where the lowest triplet level of an acceptor molecule lies below the simultaneous transition state of the singlet oxygen molecular pair may occur. Our study of the sensitized luminescence of fluorescein anion and Rose Bengal suggest that they may fit this mechanism. Then the dye fluorescence may be produced as a "delayed fluorescence" after Boltzmann activation from the sensitized triplet. The energy criteria are (cf. Fig. 12)

$$\Delta E_{\mathrm{T}_1} < 2(\Delta E_{\mathrm{1}_{\Delta_{\mathrm{g}}}})$$
  $(\Delta E_{\mathrm{S}_1} - \Delta E_{\mathrm{T}_1}) \simeq kT$   $\mathrm{S}_{\mathrm{1}}$   $\mathrm{T}_{\mathrm{1}}$   $\mathrm{T}_{\mathrm{1}}$   $\mathrm{T}_{\mathrm{2}}$   $\mathrm{T}_{\mathrm{3}}$   $\mathrm{T}_{\mathrm{2}}$   $\mathrm{T}_{\mathrm{3}}$   $\mathrm{T}_{\mathrm{2}}$   $\mathrm{T}_{\mathrm{3}}$ 

Fig. 12. Photosensitization by singlet oxygen. Mechanism c: Delayed fluorescence sensitization.

The mechanism would apply with restriction of quantum yield to the other simultaneous transition states of  $O_2$  also. The temperature dependence may be complicated because the delayed fluorescence activation will compete with temperature-dependent quenching steps.

# Mechanism d: Sensitization of Triplet-Triplet Annihilation

Triplet-triplet annihilation is a well-known phenomenon in molecular systems in condensed phases. If a large population of triplets is produced, this mechanism may be favored. We propose that the two independent

triplets are excited by the simultaneous transition states of singlet oxygen, e.g.,  $({}^{1}\Delta_{o})({}^{1}\Delta_{o})$ . Unlike the energy pooling (mechanism a) case, the energy criteria are not very restrictive (cf. Fig. 13)

$$\Delta E_{\mathrm{T_1}} < 2(\Delta E_{\mathrm{1}_{\Delta_{\mathrm{g}}}})$$
  
 $\Delta E_{\mathrm{S_1}} \gg 2(\Delta E_{\mathrm{1}_{\Delta_{\mathrm{g}}}}).$ 

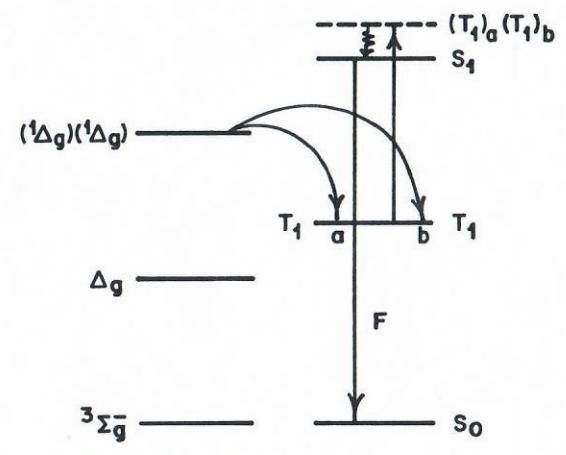


Fig. 13. Photosensitization by singlet oxygen. Mechanism d: Sensitization of triplettriplet annihilation.

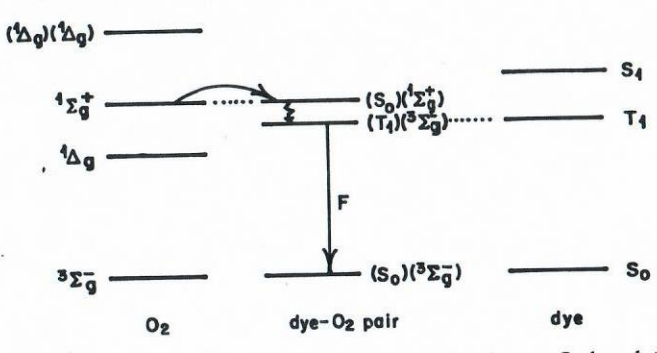
We have not yet found a case which exclusively requires this mechanism, but a careful search should reveal good examples.

#### Mechanism e: Induced Fluorescence

Recently we have uncovered an unusual case in the singlet-oxygen sensitized luminescence of methylene blue (Brabham and Kasha, 1974). Methylene blue has a fluorescence with a peak near 7000 Å, but in the presence of singlet oxygen in the hypochlorite-peroxide reaction, a new intense luminescence emission is observed with a broad band centered at 8130 Å. This emission occurs at the expected position for the triplet-singlet emission of methylene blue, although the intrinsic emission has eluded all attempts at its direct observation. In spite of this, methylene blue is known to be a good triplet sensitizer of photooxygenation. We believe this to be an example of the case described here by Fig. 14. The energetics of methylene blue fit the criterion

$$\Delta E_{\mathrm{T}_{1}} < \Delta E_{\mathrm{1}_{\Sigma_{\mathbf{g}}}}$$

## 1. Electronic St. Jeture and Sensitization



Photosensitization by singlet oxygen. Mechanism e: Induced triplet-triplet fluorescence.

We believe that the  $^1\Sigma_g^{\ +}$  state is the sensitizer, since the  $(^1\Delta_g)(^1\Delta_g)$  state emission is not affected in first-order by the yield of the new luminescence. Other thiazine dyes are progressively less efficiently excited as they fail to satisfy this energy criterion. This sensitized "triplet" -> "triplet" fluorescence in the complex [(T)(T) yields (S + T + Q) multiplicity in excited state; (S)(T) yields (T) multiplicity in ground state] must occur in competition with the back excitation of triplet dye  $\rightarrow$  normal oxygen (producing  $^{1}\Delta_{g}$ ).

## VI. SUMMARY

The electronic structure of molecular oxygen is examined at successive levels of sophistication from primitive models to antisymmetrized complex state functions and real state functions, for the  ${}^3\Sigma_g^-$ ,  ${}^1\Delta_g$ , and  ${}^1\Sigma_g^+$  states arising from the ...  $(\pi_g)^2$  configuration. The treatment is at a level permitting an experimentalist, uninitiated into the chemical physics of electron quantum mechanics, to obtain an insight into a realistic understanding of the electronic states involved in oxygen excitation and interaction. The paper concludes with the discussion of five mechanisms, differentiated by energetic and spectroscopic criteria, for photosensitization of molecules by singlet oxygen.

# **ACKNOWLEDGMENTS**

We express our thanks to W. H. Eberhardt of the Georgia Institute of Technology for calling our attention to the error in Fig. 8, Kasha and Khan (1970) noted above; to our colleagues W. Rhodes for informative discussions on complex wave function geometrical transformations, and J. Saltiel for valuable editorial critiques. We especially thank our colleague S. P. McGlynn of Louisiana State University for his penetrating technical and editorial comments. The preparation of this paper was suported by the Division of Biomedical and Environmental Research, U. S. Energy Research and Development Administration, under Contract No. EY-76-S-05-2690.

#### REFERENCES

Arnold, S. J., Ogryzlo, E. A., and Witzke, H. (1964). J. Chem. Phys. 40, 1769.

Arnold, S. J., Kubo, M., and Ogryzlo, E. A. (1968). Adv. Chem. Ser. 77, 133.

Ballhausen, C. J., and Gray, H. B. (1964). "Molecular Orbital Theory," p. 45. Benjamin, New York.

Brabham, D., and Kasha, M. (1974). Chem. Phys. Lett. 29, 159.

Browne, R. J., and Ogryzlo, E. A. (1964). Proc. Chem. Soc., London p. 117.

Ellis, J. W., and Kneser, H. O. (1933). Z. Phys. 86, 583.

Eyring, H., Walter, J., and Kimball, G. E. (1944). "Quantum Chemistry." Wiley, New York.

Gray, E. W., and Ogryzlo, E. A. (1969). Chem. Phys. Lett. 3, 658.

Griffith, J. S. (1964a). J. Chem. Phys. 40, 2899.

Griffith, J. S. (1964b). In "Oxygen in Animal Organisms" (F. Dickens and E. Neil, eds.), p. 481. Pergamon, Oxford.

Groh, P., and Kirrmann, K. A. (1942). C. R. Hebd. Seances Acad. Sci. 215, 275.

Herzberg, G. (1934). Nature (London) 133, 759.

Herzberg, G., and Herzberg, L. (1948). Astrophys. J. 108, 167.

Herzberg, L., and Herzberg, G. (1947). Astrophys. J. 105, 353.

Herzberg, G. (1950). "Molecular Spectra and Molecular Structure. I. Spectra of Diatomic Molecules," 2nd ed., p. 446. Van Nostrand-Reinhold, New York.

Hückel, E. (1930). Z. Phys. 60, 423.

Kasha, M., and Khan, A. U. (1970). Ann. N. Y. Acad. Sci. 171, 5.

Kauzmann, W. (1957). "Quantum Chemistry," Academic Press, New York.

Kawaoka, K., Khan, A. U., and Kearns, D. R. (1967). J. Chem. Phys. 46, 1842.

Kearns, D. R. (1969). J. Am. Chem. Soc. 91, 6554.

Kearns, D. R. (1971). Chem. Rev. 71, 395.

Khan, A. U., and Kasha, M. (1963). J. Chem. Phys. 39, 2105.

Khan, A. U., and Kasha, M. (1964). Nature (London) 204, 241.....

Khan, A. U., and Kasha, M. (1966). J. Am. Chem. Soc. 88, 1574.

Khan, A. U., and Kasha, M. (1970). J. Am. Chem. Soc. 92, 3293.

Khan, A. U., and Kearns, D. R. (1968). J. Chem. Phys. 48, 3272.

Kotani, M., Mizuno, Y., and Kayama, K. (1957). J. Phys. Soc. Jpn. 12, 707.

Krupenie, P. H. (1972). J. Phys. Chem. Ref. Data 1, 423.

Lennard-Jones, J. E. (1929). Trans. Faraday Soc. 25, 668.

Lewis, G. N. (1916). J. Am. Chem. Soc. 38, 762.

Lewis, G. N. (1924a). Chem. Rev. 1, 231.

Lewis, G. N. (1924b). J. Am. Chem. Soc. 46, 2027.

Long, C. A., and Kearns, D. R. (1975). J. Am. Chem. Soc. 97, 2018.

Meckler, A. (1953). J. Chem. Phys. 21, 1750.

Merkel, P. B., and Kearns, D. R. (1972). J. Am. Chem. Soc. 94, 7244.

# 1. Electronic Structure and Sensitization

Moffitt, W. (1951). Proc. R. Soc. London 210, 224.

Mulliken, R. S. (1928). Nature (London) 122, 505.

Mulliken, R. S. (1932). Rev. Mod. Phys. 4, 1 (esp. pp. 54-56, and Fig. 48).

Ogryzlo, E. A., and Pearson, E. A. (1968). J. Phys. Chem. 72, 2913.

Pauling, L. (1960). "Nature of the Chemical Bond," 2nd ed. Cornell Univ. Press, Ithaca, New

Pauling, L., and Wilson, E. B., Jr. (1935). "Introduction to Quantum Mechanics." McGraw-Hill, New York.

Schaap, A. P. (1976). "Singlet Molecular Oxygen." Dowden, Hutchinson, & Ross, Stroudsberg, Pennsylvania.

Stauff, J., and Schmidkunz, H. (1962). Z. Phys. Chem. (Frankfurt am Main) 35, 295.

Wilson, T. (1969). J. Am. Chem. Soc. 91, 2387.